Free Vibrations of a Double Layered Elastic Isotropic Cylindrical Rod

A. Charalambopoulos, D.I. Fotiadis
and C.V. Massalas

11-96

Preprint no. 11-96/1996

**Department of Computer Science
University of Ioannina
45 110 Ioannina, Greece**

FREE VIBRATIONS OF A DOUBLE LAYERED ELASTIC ISOTROPIC CYLINDRICAL ROD

A. CHARALAMBOPOULOS
Institute of Chemical Engineering and High Temperature Chemical Processes, GR 265 00 Patras, Greece

D.I. FOTIADIS
Dept. of Computer Science, University of Ioannina, GR 451 10 Ioannina Greece

and

C.V. MASSALAS*
Dept. of Mathematics, University of Ioannina, GR 451 10 Ioannina, Greece

No. of Pages: 36

No. of Tables: 5

No. of Figures: 3

* Author to whom correspondence should be addressed

SUMMARY

In this work we propose an approach to study the dynamic characteristics of cylindrical rods. The description of the problem is based on the three-dimensional theory of elasticity and the mathematical analysis on the representation of the displacement fields in terms of the constructed Navier eigenvectors in cylindical coordinates. Finally, for a special case, the proposed analysis is presented in details and the results obtained are in excellent agreement with the existing ones.

1. INTRODUCTION

The problem of free vibrations of a circular cylinder of an isotropic material was first studied in terms of the general theory of elasticity by Pochhammer 1876 and independently by Chree in 1889. An account of this treatment is given in the book by Kolsky [1]. The Pochhammer - Chree solutions are exact for infinitely long isotropic rods that are stress - free at the lateral (cylindrical) surface. However, these solutions cannot completely satisfy the boundary conditions for a finite rod since they do not permit stress - free ends. A complete solution for the axisymmetric free vibrations of a finite length isotropic cylindrical rod was given by Hutchinson [2]. His series solution can be made as accurate as required by including enough terms in the series. Tables of natural frequencies and mode shapes of infinitely long solid circular cylinders have been compiled by Armenakas et al. [3].

If the cylinder is constructed of a material with anisotropic constitutive relations, the solution of the free vibrations problem significantly increases in complexity. Morse [4] extended the Pochhammer - Chree solutions to investigate the case of an infinitely long cylinder composed of a material with hexagonal symmetry. Lusher and Hardy [5] used the approach of Morse to extend the solution technique of Hutchinson for isotropic cylinders to study the axisymmetric vibrations of a finite cylindrical rod which is transversely isotropic and compared the results with the experimental results for sapphire material . Heyliger [6] and Heyliger and Jilani [7] studied the axisymmetric vibrations of anisotropic cylinders of finite length and the free vibrations of inhomogeneous elastic cylinders, respectively by using the Ritz method. Paul and Natarajan [8] extended the Hutchinson technique to investigate the flexural vibrations of a piezoelectric finite circular cylinder of crystal class 6 mm.

The elastic wave propagation problems of long bones were investigated by Voya and Ghista [9] by assuming that the bone is made of two layered concentric hollow cylinders, where the inner part was taken as the spongy layer and the outer part was taken as the compact layer. Nowicki and Davis [10] were also analysed wave propagation in bone, treating bone as a solid poroelastic cylinder. The propagation of flexural waves in an infinite cylindrical bone element which is porous in nature was considered by Paul and Murali [11]. The electromechanical wave propagation in the diaphysis of a dry femur (long bone) due to mechanical stress waves was studied by Güzelsu and Saha [12] considering the long bone as hollow cylinder of infinite extent and using the mathematical analysis proposed by Mirsky [13].

In the present work an attempt is made to study the free vibrations problem of a double layered elastic isotropic cylindrical rod. For the purpose of our analysis we constructed the Navier vector eigenfunctions in cylindrical coordinates, for the three-dimensional theory of linear elasticity, and the solution of the problem was represented in terms of them. The selection of the specific solution from the general representation is imposed by the boundary conditions on the discontinuity surfaces. For the case of stress - free lateral surface, continuity of displacements and stress fields on the contact surface of the layers and the most simple boundary conditions on the plane boundaries, the mathematical analysis is presented in details and numerical results for the dynamic characteristics of the system considered are presented by simulating the outer layer with the space of cortical bone and the inner one with the medullary space. The cases of more realistic boundary conditions and material behaviour are in preparation.

2. PROBLEM FORMULATION

The system under consideration as well as the coordinate system are shown in Fig. 1. The inner region and the outer one of the system is supposed to be constructed of a material with isotropic constitutive relations.

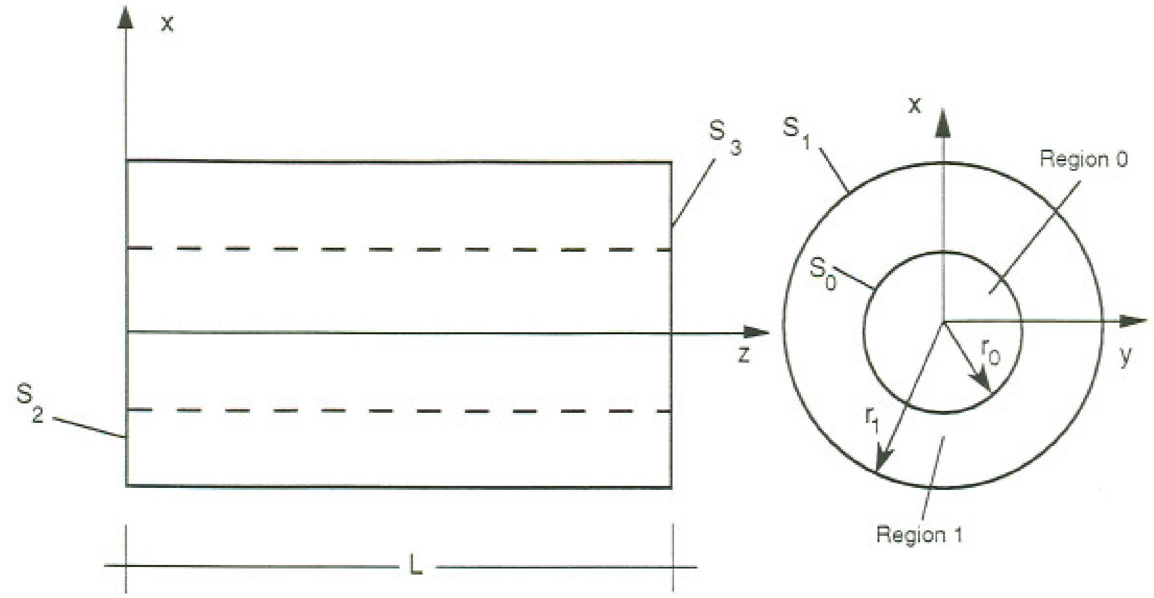

Figure 1: Problem geometry

The main purpose of the present analysis is the determination of the dynamic characteristics of the system shown in Fig. 1 under prescribed boundary conditions on the discontinuity surfaces, $S_k, k = 0,1,2,3$.

The displacement fields $\boldsymbol{u}_0(\boldsymbol{r}), \boldsymbol{u}_1(\boldsymbol{r})$ in the regions 0 and 1 satisfy, after suppressing the time-harmonic dependence, the time independent equation of elasticity

$$c_{s_i}^2 \nabla^2 \boldsymbol{u}_i(\boldsymbol{r}) + (c_{p_i}^2 - c_{s_i}^2)\nabla(\nabla \cdot \boldsymbol{u}_i(\boldsymbol{r})) + \omega^2 \boldsymbol{u}_i(\boldsymbol{r}) = \boldsymbol{0}, \ \ \boldsymbol{r} \in V_i, \ \ i = 0,1 \tag{1}$$

where ω is the eigenfrequency (rads/sec) and $c_{P_i} = \left(\dfrac{\lambda_i + 2\mu_i}{\rho_i}\right)^{1/2}$, $c_{S_i} = \left(\dfrac{\mu_i}{\rho_i}\right)^{1/2}$ are the velocities of the longitudinal and transverse waves, respectively, λ_i, μ_i are the Lamè constants and ρ_i is the density of the i - medium.

Introducing the dimensionless quantities

$$r' = \frac{r}{r_1},\ z' = \frac{z}{r_1},\ L' = \frac{L}{r_1},\ \Omega = \frac{\omega r_1}{c_{p_1}},$$

equation (1) can be written as

$$c'^2_{s_i} \nabla'^2 \boldsymbol{u}_i(\boldsymbol{r}') + (c'^2_{p_i} - c'^2_{s_i}) \nabla' (\nabla' \cdot \boldsymbol{u}_i(\boldsymbol{r}')) + \Omega^2 \boldsymbol{u}_i(\boldsymbol{r}') = \boldsymbol{0},\ \boldsymbol{r}' \in V_i,\ \ i = 0,1 \qquad (2)$$

where $\nabla' = r_1 \nabla$.

The displacement field $\boldsymbol{u}_i(\boldsymbol{r}')$ can be decomposed into the longitudinal irrotational field $\boldsymbol{u}_i^{(p)}(\boldsymbol{r}')$ and the transverse solenoidal field $\boldsymbol{u}_i^{(s)}(\boldsymbol{r}')$, which satisfy the vector Helmholtz equation with wave number , $k'_{p_i} = \Omega / c'_{p_i}$ and $k'_{s_i} = \Omega / c'_{s_i}$, respectively (see Appendix D).

The mathematical problem described by equation (1) and the appropriate boundary conditions on $S_i,\ \ i = 0,1,2,3$ consists of a well - posed mathematical problem (see section 3).

3. PROBLEM SOLUTION

Following separation variables techniques and taking advantage of irrotational and solenoidal properties of the longitudinal and transverse fields, respectively, we construct all the possible vector solutions of equation (2) (Their derivation is presented in Appendix D). These functions, which remind us the Navier vector eigenfunctions of the spherical geometry [14], are the following:

$$\boldsymbol{L}^{m,l}_{i,j}(\boldsymbol{r}' : \lambda) = \dot{\Phi}^l_m (x^j_{p_i} r') \boldsymbol{P}^m_j (\varphi, z' ; \lambda) + \frac{\Phi^l_m (x^j_{p_i} r')}{x^j_{p_i} r'} \left[im \boldsymbol{B}^m_j (\varphi, z' ; \lambda) + r' \boldsymbol{C}^m_j (\varphi, z' ; \lambda) \right] \qquad (3)$$

$$M_{i,j}^{m,l}(\boldsymbol{r}';\lambda) = \frac{\Phi_m^l(x_{s_i} r')}{x_{s_i} r'} im\boldsymbol{P}_j^m(\varphi,z';\lambda) - \dot{\Phi}_m^l(x_{s_i} r')\boldsymbol{B}_j^m(\varphi,z';\lambda) \tag{4}$$

$$\begin{aligned} N_{i,j}^{m,l}(\boldsymbol{r}';\lambda) &= (-1)^j \lambda^2 \dot{\Phi}_m^l(x_{s_i}^j r')\boldsymbol{P}_j^m(\varphi,z';\lambda) + (-1)^j im\lambda^2(n)\frac{\Phi_m^l(x_{s_i}^j r')}{x_{s_i}^j r'}\boldsymbol{B}_j^m(\varphi,z';\lambda) \\ &+ x_{s_i}^j \Phi_m^l(x_{s_i}^j r')\boldsymbol{C}_j^m(\varphi,z';\lambda) \end{aligned} \tag{5}$$

where

$$x_{S_i}^j = \begin{cases} \sqrt{k'^2_{S_i} - \lambda^2} & \text{if } j = 1,3 \\ \sqrt{k'^2_{S_i} + \lambda^2} & \text{if } j = 2,4 \end{cases}, \quad i = 0,1 \tag{6}$$

$$x_{P_i}^j = \begin{cases} \sqrt{k'^2_{P_i} - \lambda^2} & \text{if } j = 1,3 \\ \sqrt{k'^2_{P_i} + \lambda^2} & \text{if } j = 2,4 \end{cases}, \quad i = 0,1 \tag{7}$$

$$\left.\begin{aligned} \boldsymbol{P}_j^m(\varphi,z';\lambda) &= e^{im\varphi} Z_j(z';\lambda)\underline{\hat{r}} \\ \boldsymbol{B}_j^m(\varphi,z';\lambda) &= e^{im\varphi} Z_j(z';\lambda)\underline{\hat{\varphi}} \\ \boldsymbol{C}_j^m(\varphi,z';\lambda) &= e^{im\varphi} Z_j(z';\lambda)\underline{\hat{z}} \end{aligned}\right\}, \quad \mathrm{j} = 1,2,3,4 \tag{8}$$

$$\begin{aligned} Z_1(z';\lambda) &= \sin(\lambda z'), \quad Z_2(z';\lambda) = \sinh(\lambda z') \\ Z_3(z';\lambda) &= \cos(\lambda z'), \quad Z_4(z';\lambda) = \cosh(\lambda z') \end{aligned} \tag{9}$$

and

$$\Phi_m^l(x) = \begin{cases} J_m(x), & l = 1 \text{ (Bessel function)} \\ Y_m(x), & l = 2 \text{ (Neumann function)} \end{cases}$$

while $\dot{\Phi}_m^l(x)$ denotes the derivative of $\Phi_m^l(x)$ with respect to its argument.

We mention here that for the solutions with solenoidal dependence on z' - coordinate (case $j = 1,3$), the parameter λ, as increases, may render the quantities $x_{S_i}^j$ or (and) $x_{P_i}^j$ imaginary. Then the Bessel functions having in their arguments these quantities are transformed suitably to the modified Bessel functions $I_m(x)$ and $K_m(x)$. We mention here that whenever $x^j_{S_1}$, $x^j_{P_1}$ become imaginary, give rise to the real quantities $x^j_{S_1}/i$, $x^j_{P_1}/i$ which we rename to $x^j_{S_1}$, $x^j_{P_1}$, respectively, for simplicity.

Consequently, the most general representation for the displacement fields $\boldsymbol{u}_i(\boldsymbol{r}'), i = 0,1$ is given by the expressions

$$\boldsymbol{u}_o(\boldsymbol{r}') = \sum_{j=1}^{4}\sum_{m=0}^{+\infty} \int_0^{+\infty}\left[\alpha^m_{0,j}(\lambda)\boldsymbol{L}^{m,1}_{0,j}(\boldsymbol{r}';\lambda) + \beta^m_{0,j}(\lambda)\boldsymbol{M}^{m,1}_{0,j}(\boldsymbol{r}';\lambda) + \gamma^m_{0,j}(\lambda)\boldsymbol{N}^{m,1}_{n,0}(\boldsymbol{r}';\lambda)\right]d\lambda, \quad \boldsymbol{r}' \in V_0 \tag{10}$$

$$\boldsymbol{u}_1(\boldsymbol{r}') = \sum_{j=1}^{4}\sum_{m=0}^{+\infty} \int_0^{+\infty}\left[\alpha^{m,l}_{1,j}(\lambda)\boldsymbol{L}^{m,l}_{1,j}(\boldsymbol{r}';\lambda) + \beta^{m,l}_{1,j}(\lambda)\boldsymbol{M}^{m,l}_{1,j}(\boldsymbol{r}';\lambda) + \gamma^{m,l}_{1,j}(\lambda)\boldsymbol{N}^{m,l}_{1,j}(\boldsymbol{r}';\lambda)\right]d\lambda, \quad \boldsymbol{r}' \in V_1 \tag{11}$$

where, as it is obvious, the regularity of the solution near the z'-axis excludes the Neumann function Y_m from the expansion of $\boldsymbol{u}_0(\boldsymbol{r}')$.

The previous expression is the more general representation for the solution of the time-independent equation of elasticity for the specific system shown in Fig. 1. Every particular solution can be obtained from this representation by selecting the coefficients of the expansion and choosing suitable integration over the parameter λ.

The specific way of selecting the solution from the general set of functions defined by the representations (10) - (11) is imposed by the concrete boundary conditions the solution has to satisfy on the discontinuity surfaces. Every set of boundary conditions determines the particular way of mixing the several structural simple solutions participating in the integrand of the representation.

It is interesting to notice that there are "bad" boundary conditions which require the presence of every partial solution with suitable weight in the expansion, as well as "good" boundary conditions which are satisfied by a finite combination of the basic simple solutions.

In this work we consider stress - free lateral surface S_1, continuity of displacement and stress fields on S_0, and the following two sets of boundary conditions at S_2 and S_3:

i. $u_r = 0,\ u_\varphi = 0,\ \tau_{zz} = 0$

ii. $\tau_{z\varphi} = 0,\ \tau_{zr} = 0,\ u_z = 0.$

The choice of these two sets is based on the necessity to examine the most general case of "good" boundary conditions, in the sense presented above, which in addition reflect real situation occurring in medical applications where the system under investigation simulates suitably long bones.

We note that the infinite rod solution can be considered as a finite rod solution with the boundary conditions (i) or (ii).

Especially the first chosen set of boundary conditions at S_2 and S_3 is adapted perfectly to the physical properties of long bones as well as to the immobilisation procedures imposed in medical treatment of long bones diseases.

Examining further the considered boundary conditions we remark that they refer both to the lateral as well as to the transverse discontinuity surfaces. However, it is interesting to notice that the particular way the "lateral" and "transverse" boundary conditions are involved in the representations (10) - (11) of the solutions is completely different. This different "nature" of the conditions reflects the incorporated properties of the cylindrical geometry that has been adopted.

More precisely, determining the stress field on the surfaces S_2 and S_3 and considering the displacement fields given by the expressions (10) - (11), it can be shown that the necessity of satisfaction of the boundary conditions on the surfaces S_2 and S_3 discretizes the initially continuous variable λ and defines exactly one accepted value of j from the four apriori possible values. Furthermore, the transverse boundary conditions dot not provide information for the coefficients of the expansions (10) - (11).

In contrast, as it will be presented later, the "lateral" boundary conditions determine the coefficients of the expansions modulo a multiplicative constant. The physical meaning of this difference is that in cylindrical geometry, transverse conditions control the "structural" pieces of the solution, i.e., determine which terms of the representation are allowed to participate in order to construct the solution, while lateral conditions determine which is the necessary mixture of these pieces in order to build the solution.

The boundary conditions (i) and (ii) at S_2 and S_3 are satisfied if the parameter λ is chosen as

$$\begin{aligned} &\lambda = f(n) = \frac{n\pi}{L'}, \quad n = 1,2,... \\ &j = 1, \ \ Z_1(z';\lambda) = Z_n(z') = \sin\left(\frac{n\pi}{L'}z'\right), \quad n = 1,2,... \end{aligned} \tag{12a}$$

and

$$\begin{aligned} &\lambda = f(n) = \frac{n\pi}{L'}, \quad n = 0,1,2,... \\ &j = 3, \ \ Z_1(z';\lambda) = Z_n(z') = \cos\left(\frac{n\pi}{L'}z'\right), \quad n = 0,1,2,... \end{aligned} \tag{12b}$$

respectively.

In both cases the representation (10) - (11), renaming some of the quantities after the imposed discretization, takes the following form

$$u_o(r') = \sum_{n=0}^{+\infty}\sum_{m=0}^{+\infty}\left[\alpha_{n,o}^{m} L_{n,0}^{m,1}(r') + \beta_{n,0}^{m} M_{n,0}^{m,1}(r') + \gamma_{n,0}^{m} N_{n,0}^{m,1}(r')\right], \quad r' \in V_0 \tag{13}$$

$$u_1(r') = \sum_{n=0}^{+\infty}\sum_{m=0}^{+\infty}\sum_{l=1}^{2}\left[\alpha_{n,1}^{m,l} L_{n,1}^{m,l}(r') + \beta_{n,1}^{m,l} M_{n,1}^{m,l}(r') + \gamma_{n,1}^{m,l} N_{n,1}^{m,l}(r')\right], \quad r' \in V_1. \tag{14}$$

where

$$\begin{aligned} L_{n,i}^{m,l}(r') &= L_{i,j}^{m,l}(r'; f(n)) \\ M_{n,i}^{m,l}(r') &= M_{i,j}^{m,l}(r'; f(n)) \\ N_{n,i}^{m,l}(r') &= N_{i,j}^{m,l}(r'; f(n)). \end{aligned} \tag{15}$$

The values of j and $f(n)$ are given in (12) and depend on the set of the boundary conditions we choose.

The stress field on every surface is given as

$$Tu_i(r') = \left[2\mu'_i \hat{n}\cdot\nabla' + \lambda'_i \hat{n}(\nabla'\cdot) + \mu'_i \hat{n}\times\nabla'\times\right] u_i(r') \tag{16}$$

where $\hat{n}$ is the outer normal unit vector on the surface under consideration.

Using the expressions (14) and (15) in equation (2), for every lateral surface (r' = const.), we have:

$$Tu_0(r') = \sum_{n=0}^{+\infty}\sum_{m=0}^{+\infty}\begin{bmatrix} (\alpha_{n,0}^{m} A_{n,0}^{m,1}(x_{p_0} r') + \beta_{n,0}^{m} D_{n,0}^{m,1}(x_{s_0} r') + \gamma_{n,0}^{m} G_{n,0}^{m,1}(x_{s_0} r')) P_n^m(\varphi, z') \\ +(\alpha_{n,0}^{m} B_{n,0}^{m,1}(x_{p_0} r') + \beta_{n,0}^{m} E_{n,0}^{m,1}(x_{s_0} r') + \gamma_{n,0}^{m} H_{n,0}^{m,1}(x_{s_0} r')) B_n^m(\varphi, z') \\ +(\alpha_{n,0}^{m} C_{n,0}^{m,1}(x_{p_0} r') + \beta_{n,0}^{m} F_{n,0}^{m,1}(x_{s_0} r') + \gamma_{n,0}^{m} K_{n,0}^{m,1}(x_{s_0} r')) C_n^m(\varphi, z') \end{bmatrix}$$

(17)

where r' is constant in region V_0, and

$$Tu_1(r') = \sum_{n=0}^{+\infty}\sum_{m=0}^{+\infty}\sum_{l=1}^{2}\begin{bmatrix} (\alpha_{n,1}^{m,l} A_{n,1}^{m,l}(x_{p_1} r') + \beta_{n,1}^{m,l} D_{n,1}^{m,l}(x_{s_1} r') + \gamma_{n,1}^{m,l} G_{n,1}^{m,l}(x_{s_1} r')) P_n^m(\varphi, z') \\ +(\alpha_{n,1}^{m,l} B_{n,1}^{m,l}(x_{p_1} r') + \beta_{n,1}^{m,l} E_{n,1}^{m,l}(x_{s_1} r') + \gamma_{n,1}^{m,l} H_{n,1}^{m,l}(x_{s_1} r')) B_n^m(\varphi, z') \\ +(\alpha_{n,1}^{m,l} C_{n,1}^{m,l}(x_{p_1} r') + \beta_{n,1}^{m,l} F_{n,1}^{m,l}(x_{s_1} r') + \gamma_{n,1}^{m,l} K_{n,1}^{m,l}(x_{s_1} r')) C_n^m(\varphi, z') \end{bmatrix}$$

(18)

where r' is constant in region V_1.

The functions $A_{n,0}^{m,1}, B_{n,0}^{m,1}, C_{n,0}^{m,1}, ...$ appearing in equations (17) and (18) are given in Appendix A.

For every vertical surface (z' = constant), we find that:

$$Tu_0(r') = \sum_{n=0}^{+\infty}\sum_{m=0}^{+\infty}\left[\begin{array}{l}(\alpha_{n,0}^{m}Q_{n,0}^{m,1}(x_{p_0}r') + \beta_{n,0}^{m}R_{n,0}^{m,1}(x_{s_0}r') + \gamma_{n,0}^{m}S_{n,0}^{m,1}(x_{s_0}r'))\dfrac{\partial \boldsymbol{P}_n^m(\varphi,z')}{\partial z'} \\ +(\alpha_{n,0}^{m}T_{n,0}^{m,1}(x_{p_0}r') + \beta_{n,0}^{m}V_{n,0}^{m,1}(x_{s_0}r') + \gamma_{n,0}^{m}W_{n,0}^{m,1}(x_{s_0}r'))\dfrac{\partial \boldsymbol{B}_n^m(\varphi,z')}{\partial z'} \\ +(\alpha_{n,0}^{m}O_{n,0}^{m,1}(x_{p_0}r') + \beta_{n,0}^{m}X_{n,0}^{m,1}(x_{s_0}r') + \gamma_{n,0}^{m}\Theta_{n,0}^{m,1}(x_{s_0}r'))e^{im\varphi}Z_n(z')\hat{z}\end{array}\right]$$

(19)

where z' is constant in region V_0, and

$$Tu_1(r') = \sum_{n=0}^{+\infty}\sum_{m=0}^{+\infty}\sum_{l=1}^{2}\left[\begin{array}{l}(\alpha_{n,1}^{m,l}Q_{n,1}^{m,l}(x_{p_1}r') + \beta_{n,1}^{m,l}R_{n,1}^{m,l}(x_{s_1}r') + \gamma_{n,1}^{m,l}S_{n,1}^{m,l}(x_{s_1}r'))\dfrac{\partial \boldsymbol{P}_n^m(\varphi,z')}{\partial z'} \\ +(\alpha_{n,1}^{m,l}T_{n,1}^{m,l}(x_{p_1}r') + \beta_{n,1}^{m,l}V_{n,1}^{m,l}(x_{s_1}r') + \gamma_{n,1}^{m,l}W_{n,1}^{m,l}(x_{s_1}r'))\dfrac{\partial \boldsymbol{B}_n^m(\varphi,z')}{\partial z'} \\ +(\alpha_{n,1}^{m,l}O_{n,1}^{m,l}(x_{p_1}r') + \beta_{n,1}^{m,l}X_{n,1}^{m,l}(x_{s_1}r') + \gamma_{n,1}^{m,l}\Theta_{n,1}^{m,l}(x_{s_1}r'))e^{im\varphi}Z_n(z')\hat{z}\end{array}\right]$$

where z' is constant in region V_1. (20)

The functions $Q_{n,0}^{m,1}, R_{n,0}^{m,1}, S_{n,0}^{m,1}, ...$ are given in Appendix A.

As it is easily verified the set of boundary conditions at S_2 and S_3 is automatically satisfied.

The remaining boundary conditions to be satisfied are the following:

$$\left.\begin{array}{l} \boldsymbol{u}_0(\boldsymbol{r}') = \boldsymbol{u}_1(\boldsymbol{r}') \\ \boldsymbol{T}\boldsymbol{u}_0(\boldsymbol{r}') = \boldsymbol{T}\boldsymbol{u}_1(\boldsymbol{r}') \end{array}\right\}, \quad \boldsymbol{r}' \in S_0 \tag{21}$$

and

$$\boldsymbol{T}\boldsymbol{u}_1(\boldsymbol{r}') = \boldsymbol{0}, \quad \boldsymbol{r}' \in S_1. \tag{22}$$

Replacing the expressions (13) - (14), (17) - (18) into the boundary conditions (21) - (22) and using orthogonality arguments for the functions $\boldsymbol{P}_n^m, \boldsymbol{B}_n^m, \boldsymbol{C}_n^m$ we infer that for every specific pair (m,n) we get 9 X 9 homogeneous system of linear equations,

$$\boldsymbol{D}\boldsymbol{x} = \boldsymbol{0}, \tag{23}$$

where

$$x = \left[\alpha_{n,1}^{m,1}, \alpha_{n,1}^{m,2}, i\beta_{n,1}^{m,1}, i\beta_{n,1}^{m,2}, \gamma_{n,1}^{m,1}, \gamma_{n,1}^{m,2}, \alpha_{n,0}^{m}, i\beta_{n,0}^{m}, \gamma_{n,0}^{m}\right]^T$$

and the elements of matrix $\boldsymbol{D}$ are given in Appendix C.

The system of equations (23) has a non trivial solution iff

$$\det(\boldsymbol{D}) = 0. \tag{24}$$

The equation (24) will determine the eigenfrequencies corresponding to the pair (m,n). We notice here that for $n \geq 1$, the two sets of the boundary conditions lead to the same eigenvalues, corresponding though to different eigenmodes, and for $n = 0$ the second set of boundary conditions lead to eigenfrequencies corresponding to independence with respect to z' - coordinate.

As far as the eigenvectors are concerned there exists a plethora of them describing displacements or stresses on several surfaces. All of them can be determined but we choose to give the most representative eigenmodes to indicate completely the behaviour of the system in every eigenstate. First, we consider the displacement fields on the lateral surface $r' = r'_1$:

$$u_{1,r}^{n,m}(r'_1) = \sum_{l=1}^{2} \left\{ \begin{array}{l} \alpha_{n,1}^{m,l} \hat{A}_{n,1}^{m,l}(x_{P_1} r'_1) + \beta_{n,1}^{m,l} \hat{D}_{n,1}^{m,l}(x_{S_1} r'_1) \\ + \gamma_{n,1}^{m,l} \hat{G}_{n,1}^{m,l}(x_{S_1} r'_1) \end{array} \right\} e^{im\varphi} Z_n(z') \tag{25}$$

$$u_{1,\varphi}^{n,m}(r'_1) = \sum_{l=1}^{2} \left\{ \begin{array}{l} \alpha_{n,1}^{m,l} \hat{B}_{n,1}^{m,l}(x_{P_1} r'_1) + \beta_{n,1}^{m,l} \hat{E}_{n,1}^{m,l}(x_{S_1} r'_1) \\ + \gamma_{n,1}^{m,l} \hat{H}_{n,1}^{m,l}(x_{S_1} r'_1) \end{array} \right\} e^{im\varphi} Z_n(z') \tag{26}$$

$$u_{1,z}^{n,m}(r'_1) = \sum_{l=1}^{2} \left\{ \alpha_{n,1}^{m,l} \hat{C}_{n,1}^{m,l}(x_{P_1} r'_1) + \gamma_{n,1}^{m,l} \hat{K}_{n,1}^{m,l}(x_{S_1} r'_1) \right\} e^{im\varphi} Z'_n(z'). \tag{27}$$

In the sequel, we consider the displacement and the stress fields on the surfaces S_2 and S_3.

For the first set of boundary conditions we have:

$$u_{0,z}^{n,m}(z'=0) = \left[\alpha_{n,0}^{m} \hat{C}_{n,0}^{m,l}(x_{P_0} r') + \gamma_{n,0}^{m} \hat{K}_{n,0}^{m,l}(x_{S_0} r') \right] e^{im\varphi} f(n) \tag{28}$$

for $0 \leq r' \leq r'_0$,

$$u_{1,z}^{n,m}(z'=0) = \sum_{l=1}^{2} \left[\alpha_{n,1}^{m,l} \hat{C}_{n,1}^{m,l}(x_{P_1} r') + \gamma_{n,1}^{m,l} \hat{K}_{n,1}^{m,l}(x_{S_1} r') \right] e^{im\varphi} f(n) \tag{29}$$

for $r'_0 \leq r' \leq r'_1$,

$$u_{i,z}^{n,m}(z'=L') = (-1)^n u_{i,z}^{n,m}(z'=0), \quad i = 0,1, \tag{30}$$

$$\hat{\boldsymbol{r}}\cdot \boldsymbol{Tu}_0^{n,m}(z'=0)=\left[\alpha_{n,0}^{m}Q_{n,0}^{m,1}(x_{P_0}r')+\beta_{n,0}^{m}R_{n,0}^{m,1}(x_{S_0}r')+\gamma_{n,0}^{m}S_{n,0}^{m,1}(x_{S_0}r')\right]e^{im\varphi}f(n) \tag{31}$$

for $0\le r'\le r'_0$,

$$\hat{\boldsymbol{r}}\cdot \boldsymbol{Tu}_1^{n,m}(z'=0)=\sum_{l=1}^{2}\left[\alpha_{n,1}^{m,l}Q_{n,1}^{m,l}(x_{P_1}r')+\beta_{n,1}^{m,l}R_{n,1}^{m,l}(x_{S_1}r')+\gamma_{n,1}^{m,l}S_{n,1}^{m,l}(x_{S_1}r')\right]e^{im\varphi}f(n) \tag{32}$$

for $r'_0\le r'\le r'_1$,

$$\underline{\hat{\varphi}}\cdot \boldsymbol{Tu}_0^{n,m}(z'=0)=\left[\alpha_{n,0}^{m}T_{n,0}^{m,1}(x_{P_0}r')+\beta_{n,0}^{m}V_{n,0}^{m,1}(x_{S_0}r')+\gamma_{n,0}^{m}W_{n,0}^{m,1}(x_{S_0}r')\right]e^{im\varphi}f(n) \tag{33}$$

for $0\le r'\le r'_0$,

$$\underline{\hat{\varphi}}\cdot \boldsymbol{Tu}_1^{n,m}(z'=0)=\sum_{l=1}^{2}\left[\alpha_{n,1}^{m,l}T_{n,1}^{m,l}(x_{P_1}r')+\beta_{n,1}^{m,l}V_{n,1}^{m,l}(x_{S_1}r')+\gamma_{n,1}^{m,l}W_{n,1}^{m,l}(x_{S_1}r')\right]e^{im\varphi}f(n), \tag{34}$$

$$\hat{\boldsymbol{r}}\cdot \boldsymbol{Tu}_i^{n,m}(z'=L')=(-1)^n\hat{\boldsymbol{r}}\cdot \boldsymbol{Tu}_i^{n,m}(z'=0),\ \ i=0,1 \tag{35}$$

$$\underline{\hat{\varphi}}\cdot \boldsymbol{Tu}_i^{n,m}(z'=L')=(-1)^n\underline{\hat{\varphi}}\cdot \boldsymbol{Tu}_i^{n,m}(z'=0),\ \ i=0,1. \tag{36}$$

For the second set of boundary conditions we have:

$$u_{0,r}^{n,m}(z'=0)=\left[\alpha_{n,0}^{m}\hat{A}_{n,0}^{m,l}(x_{P_0}r')+\beta_{n,0}^{m}\hat{D}_{n,0}^{m,l}(x_{S_0}r')+\gamma_{n,0}^{m}\hat{G}_{n,0}^{m,l}(x_{S_0}r')\right]e^{im\varphi} \tag{37}$$

for $0\le r'\le r'_0$,

$$u_{1,r}^{n,m}(z'=0)=\sum_{l=1}^{2}\left[\alpha_{n,1}^{m,l}\hat{A}_{n,1}^{m,l}(x_{P_1}r')+\beta_{n,1}^{m,l}\hat{D}_{n,1}^{m,l}(x_{S_1}r')+\gamma_{n,1}^{m,l}\hat{G}_{n,1}^{m,l}(x_{S_1}r')\right]e^{im\varphi} \tag{38}$$

for $r'_0\le r'\le r'_1$,

$$u_{0,\varphi}^{n,m}(z'=0)=\left[\alpha_{n,0}^{m}\hat{B}_{n,0}^{m,l}(x_{P_0}r')+\beta_{n,0}^{m}\hat{E}_{n,0}^{m,l}(x_{S_0}r')+\gamma_{n,0}^{m}\hat{H}_{n,0}^{m,l}(x_{S_0}r')\right]e^{im\varphi} \tag{39}$$

for $0\le r'\le r'_0$,

$$u_{1,\varphi}^{n,m}(z'=0)=\sum_{l=1}^{2}\left[\alpha_{n,1}^{m,l}\hat{B}_{n,1}^{m,l}(x_{P_1}r')+\beta_{n,1}^{m,l}\hat{E}_{n,1}^{m,l}(x_{S_1}r')+\gamma_{n,1}^{m,l}\hat{H}_{n,1}^{m,l}(x_{S_1}r')\right]e^{im\varphi} \tag{40}$$

for $r'_0\le r'\le r'_1$,

$$u_{i,r}^{n,m}(z'=L')=(-1)^n u_{i,r}^{n,m}(z'=0),\quad i=0,1 \tag{41}$$

$$u_{i,\varphi}^{n,m}(z'=L')=(-1)^n u_{i,\varphi}^{n,m}(z'=0),\quad i=0,1, \tag{42}$$

and

$$\hat{z}\cdot \boldsymbol{Tu}_0^{n,m}(z'=0)=\left[\alpha_{n,0}^{m}O_{n,0}^{m,1}(x_{P_0}r')+\beta_{n,0}^{m}X_{n,0}^{m,1}(x_{S_0}r')+\gamma_{n,0}^{m}\Theta_{n,0}^{m,1}(x_{S_0}r')\right]e^{im\varphi}f(n) \tag{43}$$

for $0\le r'\le r'_0$,

$$\hat{z}\cdot \boldsymbol{Tu}_1^{n,m}(z'=0)=\sum_{l=1}^{2}\left[\alpha_{n,1}^{m,l}O_{n,1}^{m,l}(x_{P_1}r')+\beta_{n,1}^{m,l}X_{n,1}^{m,l}(x_{S_1}r')+\gamma_{n,1}^{m,l}\Theta_{n,1}^{m,l}(x_{S_1}r')\right]e^{im\varphi}f(n) \tag{44}$$

for $r'_0\le r'\le r'_1$,

$$\hat{z}\cdot \boldsymbol{Tu}_i^{n,m}(z'=L')=(-1)^n\hat{z}\cdot \boldsymbol{Tu}_i^{n,m}(z'=0),\quad i=0,1. \tag{45}$$

4. RESULTS

The frequency equation (24) has been solved numerically and for this purpose a matrix determinant computation routine was used for different frequency coefficients Ω, along with a bisection method to refine steps close to its roots. The root finding algorithm is followed by an LU-decomposition and back-substitution routine to determine the eigenvector $\underline{x}$ whose elements are used for the computation of the corresponding displacement components. Given that for every particular pair (m,n) we get independent linear systems, we deduce that finally the eigenvectors are obtained by (23) without the external summation over n.

The elements of $\boldsymbol{D}$ are functions of Ω (see Appendices A and B) and therefore they have to be computed for every different value of it. This fact requires the computation of Bessel and modified Bessel functions of the first and second kind as well as their derivatives. In our computations we have used Seed's method [15] for the computation of Bessel functions of fractional order and their derivatives and a method proposed in Ref. [15] for the computation of the modified Bessel functions. We note that recursive relations, although they offer flexibility and fast computations, are not valid for high order of Bessel functions and values of the argument close to zero

Since the computations were made by a bisection method, some of the roots of the frequency equation might correspond to values of Ω where $k'^2_{p_i} - f^2(n)$ or $k'^2_{s_i} - f^2(n)$ changes sign (the Bessel functions have to be substituted by modified ones). These roots are excluded since they do not correspond to eigenfrequencies of the system but they represent discontinuities of computations.

The numerical computations for the systems under discussion have been performed by assuming isotropic bone properties:

Region 1 (Cortical Bone) [16]

$E = 10.155x10^9\ N/m^2,\ \ \nu = 0.27,\ \ \rho = 2.1326x10^3\ Kg/m^3,$

Region 0 (Medullary Space) [17]

$$K = 2.1029753x10^9\, N/m^2,\ \ \rho = 1.0002x10^3\, Kg/m^3,$$

where E, K and ν denote the Young's modulus, bulk modulus and Poisson's ratio, respectively. and $\lambda = E\nu/((1+\nu)(1-2\nu))$ and $\mu = E/(2(1+\nu))$ are the Lamè's constants.

The basic geometry used in the computations is representative of long bones [12], that is:

$$r_0 = 0.008m,\ \ r_1 = 0.014m,\ \ L = 0.16m.$$

For the purpose of comparison in Table 1 we present the results of our analysis and those cited in Ref. [3].

Table 1: Comparison of $\omega^* = \Omega\sqrt{\dfrac{1-\nu}{1-2\nu}}$ with those of Ref. [3].

		Present Analysis*			Armenakas et al. [3]		
h/R	m	1st	2nd	3rd	1st	2nd	3rd
0.1	1	1.06233	2.37451	3.96341	1.06226	2.37443	3.96340
	2	0.88251	2.71589	4.48757	0.88233	2.71586	4.48741
	3	0.80946	3.15324	5.23671	0.80925	3.15325	5.23646
	4	0.89894	3.66211	6.12246	0.89877	3.66194	6.12235
0.2	1	1.18889	2.37571	3.95288	1.18889	2.37566	3.95272
	2	1.10093	2.71821	4.46603	1.10092	2.71819	4.46586
	3	1.19755	3.15670	5.19500	1.19755	3.15658	5.19492
	4	1.48937	3.66644	6.05046	1.48933	3.66639	6.05026
0.3	1	1.33732	2.37760	3.93351	1.33727	2.37754	3.93340
	2	1.32335	2.72152	4.42453	1.32335	2.72149	4.42440
	3	1.52768	3.16101	5.11174	1.52764	3.16095	5.11162
	4	1.92667	3.67056	5.90185	1.92660	3.67046	5.90169

* We note that our results coincide almost to those of Ref. [3] when a single precision arithmetic is used in the computations.

The variation of the frequency coefficient Ω as a function of the wave numbers m and n is given in Table 2, while the variation of Ω as a function of L/r_1 and r_0/r_1 for $(m,n) = (1,1)$ is shown in Table 3. From the results cited in Table 3 we observe that for $L/r_1 \leq 4$ and $r_0/r_1 \leq 0.571$ the frequency coefficient Ω decreases as L/r_1 and r_0/r_1 are increasing, and also that the frequency spectrum of the rod is significantly changed with the increment of L/r_1 and r_0/r_1.

Table 2: Eigenfrequency Coefficients $\Omega(m,n)$ for long isotropic bone.

m	n=1	n=2	n=3	n=4	n=5
m=0	0.14982	0.29831	0.42461	0.47610	0.52817
	0.21558	0.36238	0.44120	0.54992	0.58311
	0.41387	0.51854	0.60828	0.65352	0.77389
	0.59382	0.59774	0.69736	0.80371	0.83405
	0.85554	0.86390	0.89220	0.99658	1.08518
	1.07383	1.07498	1.07700	1.08016	1.13629
m=1	0.03301	0.11526	0.22014	0.33108	0.43838
	0.56109	0.57003	0.57440	0.57622	0.57963
	0.75718	0.76384	0.76893	0.77498	0.78187
	0.77716	0.84842	0.94343	1.02357	1.04875
	1.08360	1.07956	1.07826	1.26716	1.15153
	1.17421	1.19882	1.23253	1.44452	1.30012
m=2	0.43964	0.45088	0.47550	0.51736	0.57677
	0.77701	0.77783	0.77894	0.78024	0.78191
	0.96350	0.96468	0.96672	0.96964	0.97342
	1.25830	1.26294	1.26782	1.27166	1.27440
	1.45797	1.46231	1.46550	1.46904	1.47312
	1.47372	1.50168	1.54943	1.61006	1.67521
m=3	0.96937	0.96935	0.96954	0.97011	0.97108
	1.04501	1.05498	1.07231	1.15802	1.12988
	1.15186	1.15295	1.15489	1.48379	1.16435
	1.48139	1.48192	1.48274	1.67745	1.48503
	1.67403	1.67469	1.67583	1.97033	1.67959
m=4	1.15486	1.15522	1.15582	1.15669	1.15813
	1.33006	1.33089	1.33227	1.33419	1.33664
	1.68310	1.68306	1.68319	1.68360	1.68431
	1.73165	1.74025	1.75463	1.77494	1.80124
	1.87363	1.87437	1.87559	1.87748	1.88034
	2.18455	2.18494	2.18555	2.18637	2.18737

Table 3: Eigenfrequency coefficients $\Omega(m=1,n=1)$ as a function of ${}^{r_0}\!/_{r_1}$ and ${}^{L}\!/_{r_1}$.

$L/r_1 = 1$						
Cylindrical Rod	0.014	0.071	0.214	0.357	0.571	0.714
					0.56946	0.46916
						0.68981
					0.83500	0.81632
				0.90133		0.93615
					1.02553	1.06412
					1.14166	1.24252
				1.27776	1.31031	1.43477
			1.47466	1.36945	1.53135	1.61031
1.53746	1.53719	1.53079	1.52418	1.67540	1.75899	1.76753
					1.92782	1.92040
				1.99383	1.98355	1.96299
			2.07456	2.09716		2.17206
2.21876	2.21839	2.20975	2.15244		2.23110	2.23211
				2.35967	2.30746	2.42818
					2.55776	2.60274
2.75721	2.75757	2.76526	2.71039	2.63342	2.76274	2.77767
			2.88201	2.86251	2.99473	2.97734
$L/r_1 = 4$						
Cylindrical Rod	0.014	0.071	0.214	0.357	0.571	0.714
0.22258	0.22257	0.22235	0.22052	0.21668	0.20451	0.18740
						0.46105
					0.57401	0.61397
					0.76815	0.79920
				0.91141	0.92978	0.89674
			1.16994	1.08913	1.07803	1.01706
1.25826	1.25794	1.24773		1.23131	1.22747	1.18657
					1.39866	1.29521
						1.46056
			1.54563	1.59268	1.56831	1.64317
1.64262	1.64270	1.64511	1.65242	1.71168	1.78589	1.82261
				2.00679	1.95664	1.83253
			2.05114		2.04076	2.02035
				2.37094	2.27336	2.20497
				2.47769		2.40056
			2.71909		2.51229	2.58623
2.98640	2.98508	2.94154	2.95614	2.87293	2.74640	2.78190

The variations of $\Omega = \Omega(v_0)$, $\Omega(E_0)$ where the subscript "$_0$" indicates material or geometric properties of the inner cylinder, is shown in Tables 4 and 5. From the results shown in Table 4 it is clear that the variation of v_0 does not influence the pattern of the frequency spectrum of the system while that of E_0 does.

In Fig. 2 and 3 mode shapes, even and odd, (u_r, u_φ, u_z) are presented corresponding, to a certain eigenfrequency for each pair (n,m). We note that m indicates the order of the Bessel functions and n the wave number in the z - direction.

Table 4: Eigenfrequency coefficients $\Omega(m=1, n=1)$ as a function of ν_0.

ν_0 =0.2	ν_0 =0.25	ν_0 =0.3	ν_0 =0.35	ν_0 =0.4	ν_0 =0.45	ν_0 =0.48	ν_0 =0.49
0.03303	0.03303	0.03302	0.03302	0.03302	0.03302	0.03301	0.03301
0.57815	0.58816	0.59131	0.58261	0.57414	0.56591	0.56109	0.55951
0.60939	0.60027	0.60568	0.63469	0.68080	0.73663	0.75718	0.76090
0.79561	0.79076	0.78656	0.78294	0.77993	0.77776	0.77716	0.77709
0.91813	0.90375	0.89268	0.88801	0.90201	0.99867	1.08360	1.08178
1.20369	1.18015	1.15802	1.13722	1.11776	1.10109	1.17421	1.22148
1.38864	1.39201	1.38006	1.36183	1.34387	1.33468	1.36352	1.39605
1.47729	1.47854	1.50375	1.53795	1.57448	1.57384	1.55819	1.55309
1.65879	1.68539	1.66112	1.63049	1.60168	1.64696	1.77763	1.77632
1.72816	1.69390	1.73937	1.83852	1.83424	1.80638	1.92908	2.02660
1.98242	1.94364	1.90800	1.88976	2.08933	2.05449	2.03430	2.22689
2.25604	2.21105	2.16861	2.12854	2.11048	2.28701	2.27208	2.42043
2.38032	2.44639	2.41427	2.37155	2.33258	2.53546	2.51013	2.50307
2.51754	2.49212	2.61928	2.62665	2.57998	2.73560	2.74552	2.74836

Table 5: Eigenfrequency coefficients $\Omega(m=1, n=1)$ as a function of E_0.

$E = E_o x10^{-3}$	$E = E_o x10^{-2}$	$E = E_o x10^{-1}$	$E = E_o x10^{0}$	$E = E_o x10^{1}$	$E = E_o x10^{2}$
0.01726	0.03195	0.03290	0.03303	0.03350	0.03655
0.05346	0.09077	0.18860	0.58816	0.08252	0.26096
0.06170	0.11656	0.20155	0.60027	0.79466	1.21249
0.07000	0.14110	0.28630	0.79076	1.40977	1.73331
0.08653	0.15576	0.36751	0.90375	1.99838	3.85041
0.09472	0.16901	0.44598	1.18015	2.09676	4.55241
0.12775	0.19492	0.49158	1.39201	2.76427	
0.14431	0.22131	0.53210	1.47854	3.46935	
0.15260	0.29949	0.61617	1.68539		
0.16911	0.32580	0.69133	1.69390		
0.17733	0.33725	0.76378	1.94364		
0.18562	0.35198	0.77343	2.21104		
0.20213	0.37801	0.78893			
0.23514	0.40398	0.87137			

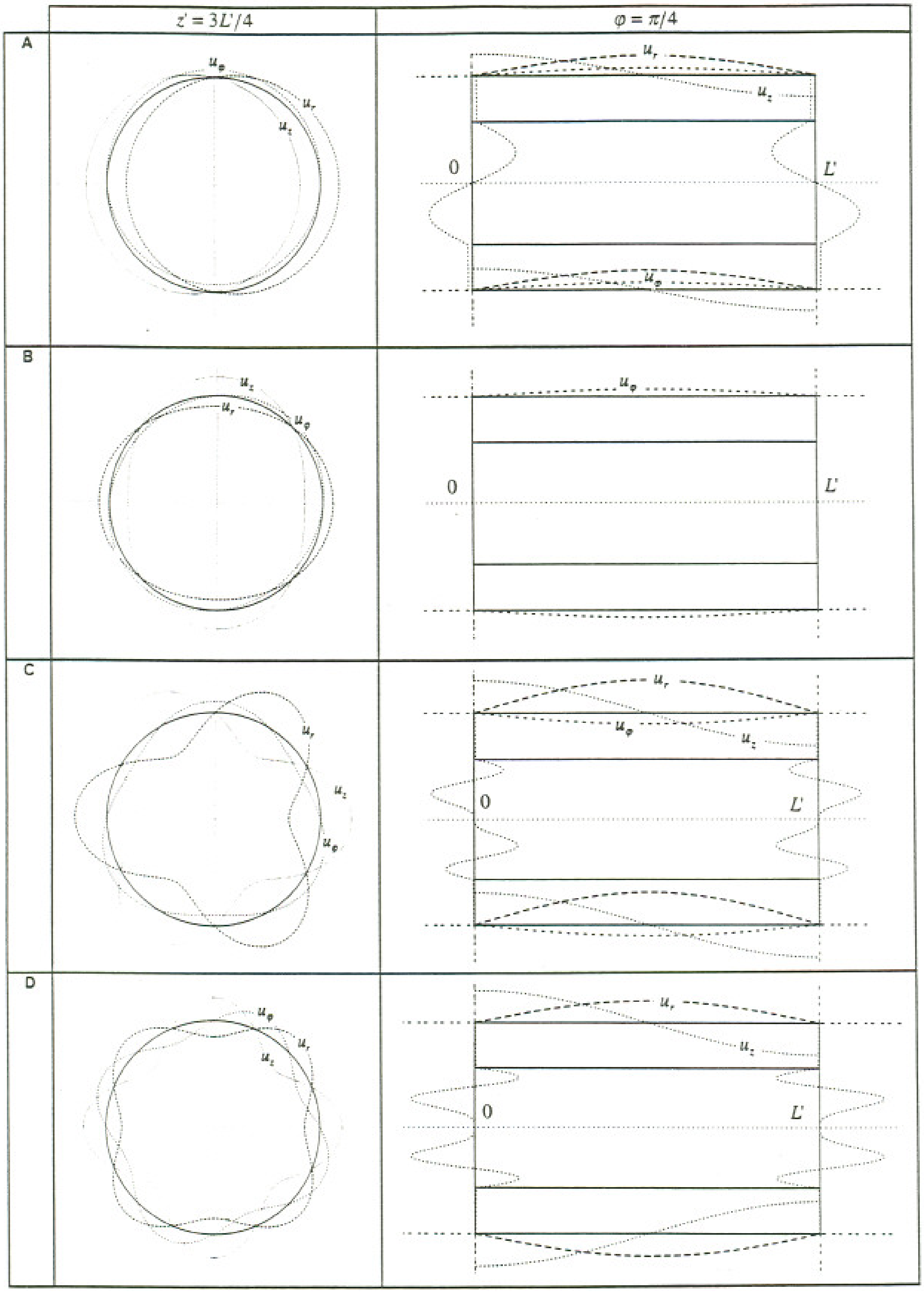

Figure 2: Mode Shapes (u_r, u_φ, u_z)
(A: $n=1$, $m=1$, $\Omega=0.56109$, B: $n=1$, $m=2$, $\Omega=0.96350$,
C: $n=1$, $m=3$, $\Omega=1.48139$, D: $n=1$, $m=4$, $\Omega=1.68310$)

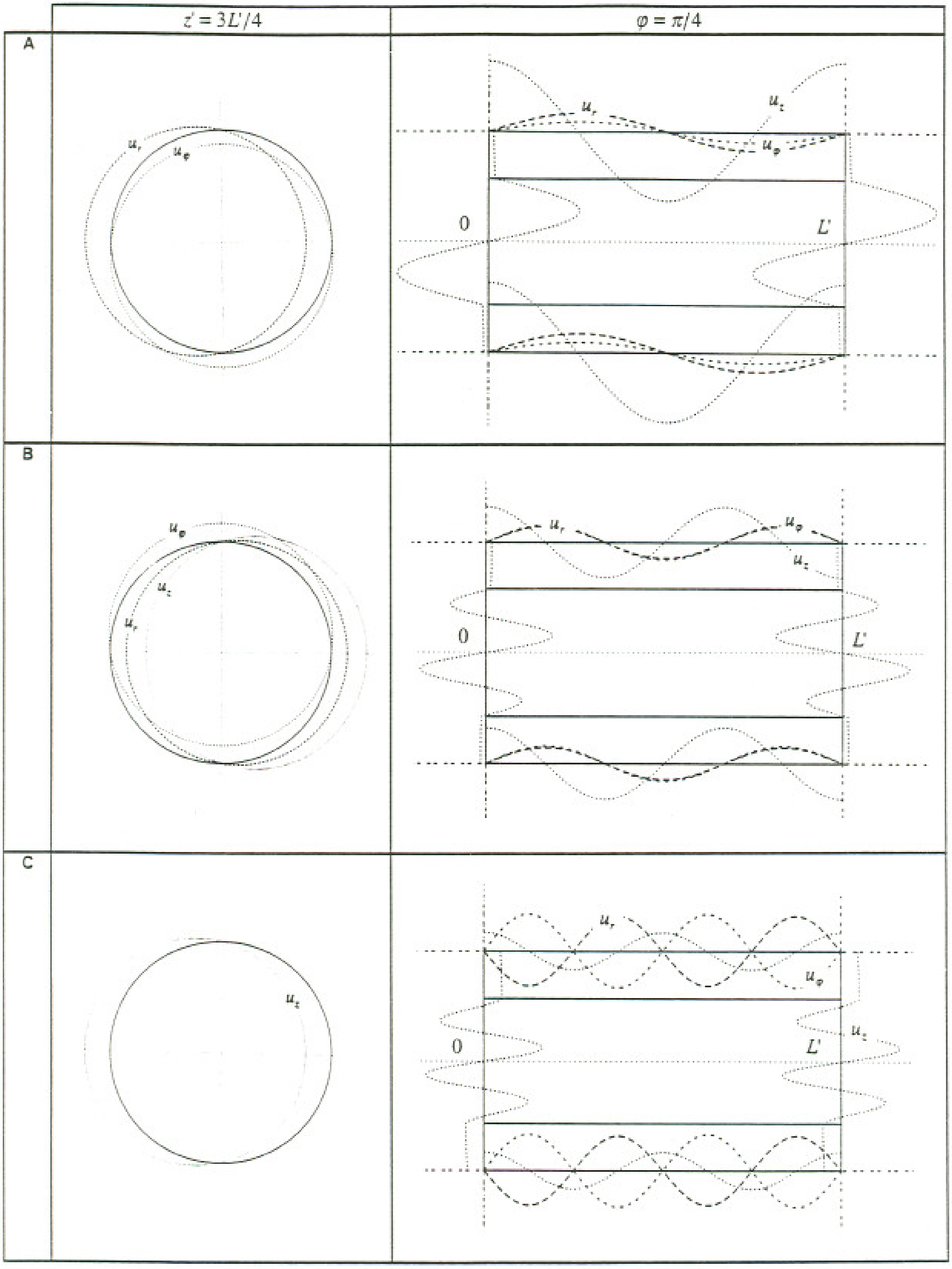

Figure 3: Mode Shpaes (u_r, u_φ, u_z)
(A: $n = 2$, $m = 1$, $\Omega = 0.76384$, B: $n = 3$, $m = 1$, $\Omega = 1.07826$,

C: $n = 4$, $m = 1$, $\Omega = 1.44452$)

5. CONCLUSIONS

In the present work, following separation of variables techniques and taking advantage of irrotational and solenoidal properties of the longitudinal and transverse fields, respectively, we constructed the Navier vector eigenfunctions of equation (2). The general representation for the solution of the time-independent equation of elasticity for the system under discussion (Fig. 1) was given in terms of the constructed Navier eigenfunctions. The selection, in each case, of the solution of the problem from the general function defined by the representation proposed is imposed by the boundary conditions. The case of stress-free lateral (cylindrical) surface, continuity of displacement and stress fields on the interface of the cylindrical surfaces and simply supported boundary conditions on the plane boundaries was presented in detail from the analytical and numerical point of view.

Especially results were presented for the eigenfrequencies and mode shapes of the system considered that are in excellent agreement with the existing ones. The proposed analysis can be used to establish limits of the validity of the shell theories. The more realistic cases with respect to the boundary conditions and material properties will be presented in a future communication.

ACKNOWLEDGEMENT

The present work forms part of the project "Development of a New Enthoprosthesis based on Bioengineering Criteria and Innovative Production Methods" which is supported by the Greek General Secretariat for Research and Technology through the EU funded R&D Program EPET II.

REFERENCES

[1] H. KOLSKY 1953 *Stress Waves in Solids*. Oxford: Clarendon Press.

[2] J.R. HUTCHINSON 1972 *Journal of the Acoustical Society of America* **51**, 233-240. Axisymmetric vibrations of a free finite length rod.

[3] A.E. ARMENAKAS, D.C. GAZIS and G. HERRMANN 1969 *Free Vibrations of Circular Cylindrical Shells*. New York: Pergamon Press.

[4] R.W. MORSE 1964 *Journal of the Acoustical Society of America* **26**, 1018-1201. Compressional waves along an anisotropic circular cylinder having hexagonal symmetry.

[5] C.P. LUSHER and W.N. HARDY 1988 *Journal of Applied Mechanics* **55**, 855-862. Axisymmetric free vibrations of a transversely isotropic finite cylindrical rod.

[6] P.R. HEYLIGER 1991 *Journal of Sound and Vibration* **148**, 507-520. Axisymmetric free vibrations of finite anisotropic cylinders.

[7] P.R. HEYLIGER and A. JILANI 1992 *Int. J. Solids and Structures* **29** **(22)**, 2689-2708. The free vibrations of inhomogeneous elastic cylinders and shapes.

[8] H.S. PAUL and K. NATARAJAN 1994 *Int. J. Engng. Sci.* **32** **(8)** 1303-1314. Flexural vibration in a finite piezoelectric circular cylinder of crystal class 6 mm.

[9] H.N. VAYO and H. GHISTA 1971 *Bull. Math. Biophys.* **33**, 463-479. Wave propagation in bone media.

[10] J. NOWINSKI and C. DAVIS 1971 *J. Appl. Mech.* **38**, 578-584. Propagation of longitudinal waves in circularly cylindrical bone elements.

[11] H.S. PAUL and V.H. MURALI 1992 *Int. J. Engng. Sci.* **30(1)** 1629-1635. Wave propagation in a cylindrical poroelastic bone with cavity.

[12] N. GÜZELSU and S. SAHA 1981 *J. of Biomechanics* **14**, 19-33. Electro-mechanical wave propagation in long bones.

[13] I. MIRSKY 1965 *Journal of Acoustical Society of America* **37(6)** 1016-1021. Wave propagation in transversely isotropic circular cylinder.

[14] A. CHARALAMBOPOULOS, G. DASSIOS, D. I. FOTIADIS, V. KOSTOPOULOS, C. V. MASSALAS 1996 *International Journal of Engineering Science*, to appear. On the dynamic characteristics of the human skull.

[15] W.H. PRESS, S.A. TEUKOLSKY, W.T. VETTERING and B.P. FLANNERY 1992 *Numerical Recipes in FORTRAN - The Art of Scientific Computing*. Cambridge: Cambridge University Press, second edition.

[16] S.B. LANG 1970 *I.E.E.E. Trans. Biomed. Engng.* **17**, 101-105. Ultrasonic method for measuring elastic coefficients of bone and results on fresh and dried bovine bones.

[17] G. VAN DER PERRE, R. VAN AUDEKERCKE, M. MARTENS and J.C. MULIER 1983 *Journal of Biomechanical Engineering TRANSACTIONS OF ASME* **105**, 244 - 248. Identification of In-Vivo Vibration Modes of Human Tibiae by Modal Analysis.

[18] J.A. STRATTON 1941. *Electromagnetic Theory*. New York: McGraw - Hill.

APPENDIX A:

For real argument we have:

$$A_{n,i}^{m,l}(x_{p_i}r') = -\left\{ \begin{array}{l} 2\mu'_i \left[\dfrac{\dot{\Phi}_m^l(x_{p_i}r')}{r'} + \left(x_{p_i} - \dfrac{m^2}{x_{p_i}r'^2} \right) \Phi_m^l(x_{p_i}r') \right] \\ +\lambda'_i k_{p_i}^2 \dfrac{1}{x_{p_i}} \Phi_m^l(x_{p_i}r') \end{array} \right\}$$

$$B_{n,i}^{m,l}(x_{p_i}r') = \frac{2\mu'_i}{r'} im \left[\dot{\Phi}_m^l(x_{p_i}r') - \frac{\Phi_m^l(x_{p_i}r')}{x_{p_i}r'} \right]$$

$$C_{n,i}^{m,l}(x_{p_i}r') = 2\mu'_i \dot{\Phi}_m^l(x_{p_i}r')$$

$$D_{n,i}^{m,l}(x_{s_i}r') = \frac{2\mu'_i}{r'} im \left[\dot{\Phi}_m^l(x_{s_i}r') - \frac{\Phi_m^l(x_{s_i}r')}{x_{s_i}r'} \right]$$

$$E_{n,i}^{m,l}(x_{s_i}r') = \mu'_i \left[\frac{2}{r'} \dot{\Phi}_m^l(x_{s_i}r') + x_{s_i} \Phi_m^l(x_{s_i}r') - \frac{2m^2}{x_{s_i}r'^2} \Phi_m^l(x_{s_i}r') \right]$$

$$F_{n,i}^{m,l}(x_{s_i}r') = \frac{\mu'_i}{x_{s_i}r'} im \Phi_m^l(x_{s_i}r')$$

$$G_{n,i}^{m,l}(x_{s_i}r') = \frac{2\mu'_i f^2(n)}{r'} \left[\begin{array}{l} \dot{\Phi}_m^l(x_{s_i}r') + x_{s_i}r' \Phi_m^l(x_{s_i}r') - \\ \dfrac{m^2}{x_{s_i}r'} \Phi_m^l(x_{s_i}r') \end{array} \right]$$

$$H_{n,i}^{m,l}(x_{s_i}r') = -\frac{2\mu'_i f^2(n)}{r'} \left[\dot{\Phi}_m^l(x_{s_i}r') - \frac{\Phi_m^l(x_{s_i}r')}{x_{s_i}r'} \right] im$$

$$K_{n,i}^{m,l}(x_{s_i}r') = \mu'_i \left[k'^2_{s_i} - 2f^2(n) \right] \dot{\Phi}_m^l(x_{s_i}r')$$

$$Q_{n,i}^{m,l}(x_{p_i}r') = 2\mu'_i \dot{\Phi}_m^l(x_{p_i}r')$$

$$T_{n,i}^{m,l}(x_{p_i}r') = 2\mu'_i im \frac{\Phi_m^l(x_{p_i}r')}{x_{p_i}r'}$$

$$O_{n,i}^{m,l}(x_{p_i}r') = -\left[2\mu'_i \frac{f^2(n)}{x_{p_i}} + \lambda'_i \frac{k'^2_{p_i}}{x_{p_i}} \right] \Phi_m^l(x_{p_i}r')$$

$$R_{n,i}^{m,l}(x_{S_i}r') = \mu'_i \frac{\Phi_m^l(x_{S_i}r')}{x_{S_i}r'} im$$

$$V_{n,i}^{m,l}(x_{S_i}r') = -\mu'_i \dot{\Phi}_m^l(x_{S_i}r')$$

$$X_{n,i}^{m,l}(x_{S_i}r') = 0$$

$$S_{n,i}^{m,l}(x_{S_i}r') = \mu'_i \dot{\Phi}_m^l(x_{S_i}r')(k'^2_{s_i} - 2f^2(n))$$

$$W_{n,i}^{m,l}(x_{S_i}r') = \mu'_i \frac{\Phi_m^l(x_{S_i}r')}{x_{S_i}r'} im(k'^2_{s_i} - 2f^2(n))$$

$$\Theta_{n,i}^{m,l}(x_{S_i}r') = -x_{s_i} f^2(n) \Phi_m^l(x_{S_i}r')$$

where Φ_m^l are the Bessel functions.

For imaginary argument we have:

$$A_{n,i}^{m,l}(x_{p_i}r') = -i^{m+1} \left\{ \begin{array}{l} 2\mu'_i \left[-\frac{\dot{\Phi}_m^l(x_{p_i}r')}{r'} + \left(x_{p_i} + \frac{m^2}{x_{p_i}r'^2} \right) \Phi_m^l(x_{p_i}r') \right] \\ -\lambda'_i k_{p_i}^2 \frac{1}{x_{p_i}} \Phi_m^l(x_{p_i}r') \end{array} \right\}$$

$$B_{n,i}^{m,l}(x_{p_i}r') = i^m \frac{2\mu'_i}{r'} m \left[\dot{\Phi}_m^l(x_{p_i}r') - \frac{\Phi_m^l(x_{p_i}r')}{x_{p_i}r'} \right]$$

$$C_{n,i}^{m,l}(x_{p_i}r') = -i^{m+1} 2\mu'_i \dot{\Phi}_m^l(x_{p_i}r')$$

$$D_{n,i}^{m,l}(x_{s_i}r') = i^m \frac{2\mu'_i}{r'} m \left[\dot{\Phi}_m^l(x_{s_i}r') - \frac{\Phi_m^l(x_{s_i}r')}{x_{s_i}r'} \right]$$

$$E_{n,i}^{m,l}(x_{s_i}r') = -i^{m+1}\mu'_i \left[\frac{2}{r'} \dot{\Phi}_m^l(x_{s_i}r') - x_{s_i} \Phi_m^l(x_{s_i}r') - \frac{2m^2}{x_{S_i}r'^2} \Phi_m^l(x_{s_i}r') \right]$$

$$F_{n,i}^{m,l}(x_{s_i}r') = i^m \frac{\mu'_i}{x_{s_i}r'} m \Phi_m^l(x_{s_i}r')$$

$$G_{n,i}^{m,l}(x_{s_i}r') = i^{m+1} \frac{2\mu'_i f^2(n)}{r'} \left[-\dot{\Phi}_m^l(x_{s_i}r') + x_{s_i}r' \Phi_m^l(x_{s_i}r') + \frac{m^2}{x_{s_i}r'} \Phi_m^l(x_{s_i}r') \right]$$

$$H_{n,i}^{m,l}(x_{s_i}r') = -i^m \frac{2\mu'_i f^2(n)}{r'}\left[\dot{\Phi}_m^l(x_{s_i}r') - \frac{\Phi_m^l(x_{s_i}r')}{x_{s_i}r'}\right]m$$

$$K_{n,i}^{m,l}(x_{s_i}r') = -i^{m+1}\mu'_i\left[k'^2_{s_i} - 2f^2(n)\right]\dot{\Phi}_m^l(x_{s_i}r')$$

$$Q_{n,i}^{m,l}(x_{p_i}r') = -2\mu'_i i^{m+1}\dot{\Phi}_m^l(x_{p_i}r')$$

$$T_{n,i}^{m,l}(x_{p_i}r') = 2\mu'_i i^m m \frac{\Phi_m^l(x_{p_i}r')}{x_{p_i}r'}$$

$$O_{n,i}^{m,l}(x_{p_i}r') = -\left[2\mu'_i \frac{f^2(n)}{x_{p_i}} + \lambda'_i \frac{k'^2_{p_i}}{x_{p_i}}\right] i^{m-1}\Phi_m^l(x_{p_i}r')$$

$$R_{n,i}^{m,l}(x_{S_i}r') = \mu'_i \frac{\Phi_m^l(x_{S_i}r')}{x_{S_i}r'} i^m m$$

$$V_{n,i}^{m,l}(x_{S_i}r') = \mu'_i i^{m+1}\dot{\Phi}_m^l(x_{S_i}r')$$

$$X_{n,i}^{m,l}(x_{S_i}r') = 0$$

$$S_{n,i}^{m,l}(x_{S_i}r') = -\mu'_i i^{m+1}\dot{\Phi}_m^l(x_{S_i}r')(k'^2_{s_i} - 2f^2(n))$$

$$W_{n,i}^{m,l}(x_{S_i}r') = \mu'_i \frac{\Phi_m^l(x_{S_i}r')}{x_{S_i}r'} i^m m(k'^2_{s_i} - 2f^2(n))$$

$$\Theta_{n,i}^{m,l}(x_{S_i}r') = -x_{s_i} i^{m+1} f^2(n)\Phi_m^l(x_{S_i}r')$$

where Φ_m^l are the modified Bessel functions.

APPENDIX B:

For real argument we have:

$$\hat{A}_{n,i}^{m,l}(x_{p_i}r') = \dot{\Phi}_m^l(x_{p_i}r')$$

$$\hat{B}_{n,i}^{m,l}(x_{p_i}r') = im \frac{\Phi_m^l(x_{p_i}r')}{x_{p_i}r'}$$

$$\hat{C}_{n,i}^{m,l}(x_{p_i}r') = \frac{\Phi_m^l(x_{p_i}r')}{x_{p_i}}$$

$$\hat{D}^{m,l}_{n,i}(x_{S_i}r') = im\frac{\Phi^l_m(x_{S_i}r')}{x_{S_i}r'}$$

$$\hat{E}^{m,l}_{n,i}(x_{S_i}r') = -\dot{\Phi}^l_m(x_{S_i}r')$$

$$\hat{F}^{m,l}_{n,i}(x_{S_i}r') = 0$$

$$\hat{G}^{m,l}_{n,i}(x_{S_i}r') = -f^2(n)\dot{\Phi}^l_m(x_{S_i}r')$$

$$\hat{H}^{m,l}_{n,i}(x_{S_i}r') = -imf^2(n)\frac{\Phi^l_m(x_{S_i}r')}{x_{S_i}r'}$$

$$\hat{K}^{m,l}_{n,i}(x_{S_i}r') = x_{S_i}\Phi^l_m(x_{S_i}r')$$

where Φ^l_m are the Bessel functions.

For imaginary argument we have:

$$\hat{A}^{m,l}_{n,i}(x_{p_i}r') = -i^{m+1}\dot{\Phi}^l_m(x_{p_i}r')$$

$$\hat{B}^{m,l}_{n,i}(x_{p_i}r') = i^m m\frac{\Phi^l_m(x_{p_i}r')}{x_{p_i}r'}$$

$$\hat{C}^{m,l}_{n,i}(x_{p_i}r') = -i^{m+1}\frac{\Phi^l_m(x_{p_i}r')}{x_{p_i}}$$

$$\hat{D}^{m,l}_{n,i}(x_{S_i}r') = i^m m\frac{\Phi^l_m(x_{S_i}r')}{x_{S_i}r'}$$

$$\hat{E}^{m,l}_{n,i}(x_{S_i}r') = i^{m+1}\dot{\Phi}^l_m(x_{S_i}r')$$

$$\hat{F}^{m,l}_{n,i}(x_{S_i}r') = 0$$

$$\hat{G}^{m,l}_{n,i}(x_{S_i}r') = i^{m+1}f^2(n)\dot{\Phi}^l_m(x_{S_i}r')$$

$$\hat{H}^{m,l}_{n,i}(x_{S_i}r') = -i^m mf^2(n)\frac{\Phi^l_m(x_{S_i}r')}{x_{S_i}r'}$$

$$\hat{K}^{m,l}_{n,i}(x_{S_i}r') = i^m x_{S_i}\Phi^l_m(x_{S_i}r')$$

where Φ_m^{l} are the modified Bessel functions.

APPENDIX C:

$$
\begin{aligned}
&d_{1,1} = A_{n,1}^{m,1}(x_{P_1} r_1),\ d_{1,2} = A_{n,1}^{m,2}(x_{P_1} r_1),\ d_{1,3} = D_{n,1}^{m,1}(x_{S_1} r_1)/i,\ d_{1,4} = D_{n,1}^{m,2}(x_{S_1} r_1)/i,\\
&d_{1,5} = G_{n,1}^{m,1}(x_{S_1} r_1),\ d_{1,6} = G_{n,1}^{m,2}(x_{S_1} r_1),\ d_{2,1} = B_{n,1}^{m,1}(x_{P_1} r_1)/i,\ d_{2,2} = B_{n,1}^{m,2}(x_{P_1} r_1)/i,\\
&d_{2,3} = -E_{n,1}^{m,1}(x_{S_1} r_1),\ d_{2,4} = -E_{n,1}^{m,2}(x_{S_1} r_1),\ d_{2,5} = H_{n,1}^{m,1}(x_{S_1} r_1),\ d_{2,6} = H_{n,1}^{m,2}(x_{S_1} r_1),\\
&d_{3,1} = C_{n,1}^{m,1}(x_{P_1} r_1),\ d_{3,2} = C_{n,1}^{m,2}(x_{P_1} r_1),\ d_{3,3} = F_{n,1}^{m,1}(x_{S_1} r_1)/i,\ d_{3,4} = F_{n,1}^{m,2}(x_{S_1} r_1)/i,\\
&d_{3,5} = K_{n,1}^{m,1}(x_{S_1} r_1),\ d_{3,6} = K_{n,1}^{m,2}(x_{S_1} r_1),\ d_{4,1} = A_{n,1}^{m,1}(x_{P_1} r_0),\ d_{4,2} = A_{n,1}^{m,2}(x_{P_1} r_0),\\
&d_{4,3} = D_{n,1}^{m,1}(x_{S_1} r_0)/i,\ d_{4,4} = D_{n,1}^{m,2}(x_{S_1} r_0)/i,\ d_{4,5} = G_{n,1}^{m,1}(x_{S_1} r_0),\ d_{4,6} = G_{n,1}^{m,2}(x_{S_1} r_0),\\
&d_{4,7} = -A_{n,0}^{m,1}(x_{P_0} r_0),\ d_{4,8} = -D_{n,0}^{m,1}(x_{S_0} r_0)/i,\ d_{4,9} = -G_{n,0}^{m,1}(x_{S_0} r_0),\ d_{5,1} = B_{n,1}^{m,1}(x_{P_1} r_0)/i,\\
&d_{5,2} = B_{n,1}^{m,2}(x_{P_1} r_0)/i,\ d_{5,3} = -E_{n,1}^{m,1}(x_{S_1} r_0),\ d_{5,4} = -E_{n,1}^{m,2}(x_{S_1} r_0),\ d_{5,5} = H_{n,1}^{m,1}(x_{S_1} r_0)/i,\\
&d_{5,6} = H_{n,1}^{m,2}(x_{S_1} r_0)/i,\ d_{5,7} = -B_{n,0}^{m,1}(x_{P_0} r_0)/i,\ d_{5,8} = E_{n,0}^{m,1}(x_{S_0} r_0),\ d_{5,9} = -H_{n,0}^{m,1}(x_{S_0} r_0)/i,\\
&d_{6,1} = C_{n,1}^{m,1}(x_{P_1} r_0),\ d_{6,2} = C_{n,1}^{m,2}(x_{P_1} r_0),\ d_{6,3} = F_{n,1}^{m,1}(x_{S_1} r_0)/i,\ d_{6,4} = F_{n,1}^{m,2}(x_{S_1} r_0)/i,\\
&d_{6,5} = K_{n,1}^{m,1}(x_{S_1} r_0),\ d_{6,6} = K_{n,1}^{m,2}(x_{S_1} r_0),\ d_{6,7} = -C_{n,0}^{m,1}(x_{P_0} r_0),\ d_{6,8} = -F_{n,0}^{m,1}(x_{S_0} r_0)/i,\\
&d_{6,9} = -K_{n,0}^{m,1}(x_{S_0} r_0),\ d_{7,1} = \hat{A}_{n,1}^{m,1}(x_{P_1} r_0),\ d_{7,2} = \hat{A}_{n,1}^{m,2}(x_{P_1} r_0),\ d_{7,3} = \hat{D}_{n,1}^{m,1}(x_{S_1} r_0),\\
&d_{7,4} = \hat{D}_{n,1}^{m,2}(x_{S_1} r_0)/i,\ d_{7,5} = \hat{G}_{n,1}^{m,1}(x_{S_1} r_0),\ d_{7,6} = \hat{G}_{n,1}^{m,2}(x_{S_1} r_0),\ d_{7,7} = -\hat{A}_{n,0}^{m,1}(x_{P_0} r_0),\\
&d_{7,8} = -\hat{D}_{n,0}^{m,1}(x_{S_0} r_0)/i,\ d_{7,9} = -\hat{G}_{n,0}^{m,1}(x_{S_0} r_0),\ d_{8,1} = \hat{B}_{n,1}^{m,1}(x_{P_1} r_0)/i,\ d_{8,2} = \hat{B}_{n,1}^{m,2}(x_{P_1} r_0)/i,\\
&d_{8,3} = -\hat{E}_{n,1}^{m,1}(x_{S_1} r_0),\ d_{8,4} = -\hat{E}_{n,1}^{m,2}(x_{S_1} r_0),\ d_{8,5} = \hat{H}_{n,1}^{m,1}(x_{S_1} r_0)/i,\ d_{8,6} = \hat{H}_{n,1}^{m,2}(x_{S_1} r_0)/i,\\
&d_{8,7} = -\hat{B}_{n,0}^{m,1}(x_{P_0} r_0)/i,\ d_{8,8} = \hat{E}_{n,0}^{m,1}(x_{S_0} r_0),\ d_{8,9} = -\hat{H}_{n,0}^{m,1}(x_{S_0} r_0)/i,\ d_{9,1} = \hat{C}_{n,1}^{m,1}(x_{P_1} r_0),\\
&d_{9,2} = \hat{C}_{n,1}^{m,2}(x_{P_1} r_0),\ d_{9,3} = \hat{F}_{n,1}^{m,1}(x_{S_1} r_0)/i,\ d_{9,4} = \hat{F}_{n,1}^{m,2}(x_{S_1} r_0)/i,\ d_{9,5} = \hat{K}_{n,1}^{m,1}(x_{S_1} r_0),\\
&d_{9,6} = \hat{K}_{n,1}^{m,2}(x_{S_1} r_0),\ d_{9,7} = -\hat{C}_{n,0}^{m,1}(x_{P_0} r_0),\ d_{9,8} = -\hat{F}_{n,0}^{m,1}(x_{S_0} r_0)/i,\ d_{9,9} = -\hat{K}_{n,0}^{m,1}(x_{S_0} r_0)
\end{aligned}
$$

In the case of imaginary argument, division by i^{m-1} of the elements of the matrix results to a real matrix.

APPENDIX D: Navier Eigenvectors in Cylindrical Coordinates

It can be proved that the displacement field $\boldsymbol{u}(\boldsymbol{r}')$ is decomposed as follows

$$\boldsymbol{u}(\boldsymbol{r}') = \boldsymbol{u}^P(\boldsymbol{r}') + \boldsymbol{u}^S(\boldsymbol{r}') \quad \text{(i)}$$

where

$$\nabla^2 \boldsymbol{u}^P(\boldsymbol{r}') + {k'_P}^2 \boldsymbol{u}^P(\boldsymbol{r}') = \boldsymbol{0} \quad \text{(ii)}$$

$$\nabla^2 \boldsymbol{u}^S(\boldsymbol{r}') + {k'_S}^2 \boldsymbol{u}^S(\boldsymbol{r}') = \boldsymbol{0} \quad \text{(iii)}$$

and

$$k'_P = \Omega, \; k'_S = \frac{\Omega}{c'_S}.$$

The transverse field $\boldsymbol{u}^S(\boldsymbol{r}')$ is proved to be solenoidal while the longitudinal $\boldsymbol{u}^P(\boldsymbol{r}')$ is irrotational. Thus, there exists a scalar function $\Psi^P(\boldsymbol{r}')$ such that $\boldsymbol{u}^P(\boldsymbol{r}') = \nabla' \Psi(\boldsymbol{r}')$. Introducing this expression in equation (ii) and using that the operators ∇' and ∇'^2 commute with each other, we conclude that the function $\Psi^P(\boldsymbol{r}')$ is obliged to satisfy the scalar Helmholtz equation with the same wave number k'_P.

The solenoidal character of the transverse field imposes that two possible forms of the displacement field $\boldsymbol{u}^S(\boldsymbol{r}')$ exist: $\nabla' \Psi^S \times \hat{a}$ and $\nabla' \times (\nabla' \Psi^S \times \hat{a})$ where Ψ^S satisfies again the scalar Helmholtz equation with wave number k'_S. The vector $\hat{\boldsymbol{a}}$ is in general an arbitrary constant unit vector [18].

We must determine the most general functions Ψ^P and Ψ^S introduced previously and replace them in the already mentioned expressions of $\boldsymbol{u}^P$ and $\boldsymbol{u}^S$ in order to get all possible forms of the displacement fields and to construct a complete set of vector eigenfunctions for the equation of elasticity.

The functions Ψ^r, $r = p,s$, having oscillatory behaviour towards z' - axis, have the form

$$\Psi_i^{m,l,t}(\mathbf{r}';\lambda) = \Phi_m^l(x_{t_i}^j r')e^{im\varphi}Z_j(z';\lambda) \qquad \text{(iv)}$$

where $t = P,S$ for the longitudinal and the transverse field, respectively, $m = 0,1,2,\ldots$,

$$\Phi_m^l(x) = \begin{cases} \begin{cases} J_m(x), & \text{for } x \in R \\ I_m(x), & \text{for } x \in Z' \end{cases}, & \text{if } l = 1 \\ \begin{cases} Y_m(x), & \text{for } x \in R \\ K_m(x), & \text{for } x \in Z' \end{cases}, & \text{if } l = 2 \end{cases}$$

$j = 1,2,3,4,\quad \lambda \in \mathrm{R}^+$ with

$Z_1(z';\lambda) = \sin(\lambda z')$, $\quad Z_2(z';\lambda) = \sinh(\lambda z')$, $\quad Z_3(z';\lambda) = \cos(\lambda z')$, $Z_4(z';\lambda) = \cosh(\lambda z')$,

$i = 0,1$ (the two elastic regions under consideration)

and $x_{t_i} = \begin{cases} \sqrt{k'^2_{t_i} - \lambda^2}, & \text{if } j = 1,3 \\ \sqrt{k'^2_{t_i} + \lambda^2}, & \text{if } j = 2,4 \end{cases}$.

Applying the procedure described previously, after selecting $\hat{a} = \hat{z}$ as it is induced by the cylindrical geometry of the problem, we get the expressions (3), (4), (5).

For the specific problem, we discuss, the boundary conditions discretize the parameter $\lambda = f(n)$, select $j = 1$ and restrict the family of allowed scalar functions presented previously, denoted now as $\Psi_{n,i}^{m,l,t}(\mathbf{r}')$.

The above functions are derived after application of separation of variables to the scalar Helmholtz equation in cylindrical coordinates.

The application of the operator $\frac{1}{x_{p_i}}\nabla'$ on $\Psi^{m,l,p}_{n,i}$ produces the first set of vector eigenfunctions:

$$L^{m,l}_{n,i}(r') = \dot{\Phi}^{l}_{m}(x_{p_i} r') P^{m}_{n}(\varphi,z') + \frac{\Phi^{m}_{n}(x_{p_i} r')}{x_{p_i} r'}\left[imB^{m}_{n}(\varphi,z') + r' C^{m}_{n}(\varphi,z')\right]. \quad \text{(v)}$$

The functions $P^{m}_{n}, B^{m}_{n}, C^{m}_{n}$, given by the expression (8) and appearing in the equation (5), constitute a symbolism reminding us the corresponding perpendicular functions of spherical geometry.

To obtain the remaining vector Navier eigenfunctions we use the scalar functions Ψ^{s}, that is:

$$M^{m,l}_{n,i}(r') = \frac{1}{x_{S_i}}\nabla\Psi^{m,l,S}_{n,i} \times \hat{z} =$$
$$\frac{\Phi^{l}_{m}(x_{S_i} r')}{x_{S_i} r'} imP^{m}_{n}(\varphi,z') - \dot{\Phi}^{l}_{m}(x_{S_i} r') B^{m}_{n}(\varphi,z') \quad \text{(vi)}$$

and

$$N^{m,l}_{n,i}(r') = \frac{1}{x_{S_i}}\nabla \times (\nabla\Psi^{m,l,S}_{n,i} \times \hat{z}). \quad \text{(vii)}$$

Instead of using $N^{m,l}_{n,i}$ we construct a new vector function $\frac{\partial}{\partial z'}N^{m,l}_{n,i}$ which satisfies also the vector Helmholtz equation (the operator $\frac{\partial}{\partial z'}$ commutes with ∇'^{2}) and constitutes a vector function independent of $M^{m,l}_{n,i}$. We prefer $\frac{\partial}{\partial z'}N^{m,l}_{n,i}$ to $N^{m,l}_{n,i}$ because the former leads to an expression dependent on the vector functions $\boldsymbol{P}_n^m, \boldsymbol{B}_n^m, \boldsymbol{C}_n^m$ instead of the latter which does not so. Renaming $\frac{\partial}{\partial z'}\boldsymbol{N}_{n,i}^{m,l}$ to $\boldsymbol{N}_{n,i}^{m,l}$, we finally have:

$$\boldsymbol{N}_{n,i}^{m,l}(\boldsymbol{r}') = \frac{1}{x'_{S_i}}\frac{\partial}{\partial z'}\nabla\times(\nabla\Psi_{n,i}^{m,l,S}\times\hat{z})$$

$$= \frac{1}{x'_{S_i}}\frac{\partial}{\partial z'}\left[\frac{\partial}{\partial z'}\nabla\Psi_{n,i}^{m,l,S} - \hat{z}\nabla'^2\Psi_{n,i}^{m,l,S}\right]$$

$$= \frac{1}{x'_{S_i}}\left[-\left(\frac{n\pi}{L'}\right)^2\nabla\Psi_{n,i}^{m,l,S} + k'_{S_i}\hat{z}\Psi_{n,i}^{m,l,S}\right]$$

$$= -\left(\frac{n\pi}{L'}\right)^2\dot{\Phi}_m^l(x_{S_i}r')\boldsymbol{P}_n^m(\varphi,z') - im\left(\frac{n\pi}{L'}\right)^2\frac{\Phi_m^l(x_{S_i}r')}{x_{S_i}r'}\boldsymbol{B}_n^m(\varphi,z')$$

$$+x_{S_i}\Phi_m^l(x_{S_i}r')\boldsymbol{C}_n^m(\varphi,z')$$